



Evaluation of thyroid nodules by shear wave elastography: a review of current knowledge

K. Z. Swan^{1,2} · V. E. Nielsen³ · S. J. Bonnema⁴

Received: 2 November 2020 / Accepted: 4 April 2021 / Published online: 16 April 2021
© Italian Society of Endocrinology (SIE) 2021

Abstract

Purpose Shear wave elastography (SWE), as a tool for diagnosing thyroid malignancy, has gathered considerable attention during the past decade. Diverging results exist regarding the diagnostic performance of thyroid SWE.

Methods A comprehensive literature review of thyroid SWE was conducted using the terms “Thyroid” and “shear wave elastography” in PubMed.

Results The majority of studies found SWE promising for differentiating malignant and benign thyroid nodules on a group level, whereas results are less convincing on the individual level due to huge overlap in elasticity indices. Further, there is lack of consensus on the optimum outcome reflecting nodule elasticity and the cut-off point predicting thyroid malignancy. While heterogeneity between studies hinders a clinically meaningful meta-analysis, the results are discussed in a clinical perspective with regard to applicability in clinical practice as well as methodological advantages and pitfalls of this technology.

Conclusion Technological as well as biological hindrances seem to exist for SWE to be clinically reliable in assessing benign and malignant thyroid nodules. Structural heterogeneity of thyroid nodules in combination with operator-dependent factors such as pre-compression and selection of scanning plane are likely explanations for these findings. Standardization and consensus on the SWE acquisition process applied in future studies are needed for SWE to be considered a clinically reliable diagnostic tool for detection of thyroid cancer.

Keywords Thyroid · Review · Diagnosis · Thyroid nodules · Thyroid carcinoma

Introduction

Thyroid nodular disease is a frequent condition, more common in women than in men, and increases with age [1]. The majority of thyroid nodules are benign, with malignancy rates of less than 5–10% [2, 3]. Differentiated thyroid carcinomas (DTC) encompass papillary thyroid carcinoma (PTC) and follicular thyroid carcinoma (FTC), and account for >90% of primary thyroid carcinoma [4]. DTC has a

favorable prognosis and a high cure rate following treatment [4, 5]. However, recurrence is seen in 20–30% of patients followed for 10–20 years [6–9].

The main goal of the diagnostic work-up of thyroid nodules is to rule out malignancy. A multi-disciplinary risk-stratification system is applied to assess functional and morphological characteristics of the thyroid as well as the risk of malignancy [3, 10, 11]. The cornerstones of thyroid nodule diagnostics are ultrasonography (US) and fine needle aspiration biopsy (FNAB). Patient selection for these methods follows an assessment of clinical risk factors for thyroid malignancy, including objective findings, thyroid function tests, and the result of ⁹⁹Tc-scintigraphy [3, 11]. The indication for FNAB is based on a risk assessment of certain US features suggestive of malignancy, while the results of FNAB triage the patients into a management strategy according to the Bethesda System for Reporting Thyroid Cytopathology (BSRTC) [10, 12, 13]. However, in a significant subset of patients, preoperative tests cannot distinguish malignant from benign nodules, and in these cases, thyroid surgery is

✉ K. Z. Swan
Kristineswan@dadlnet.dk

¹ Department of Oto-Rhino-Laryngology, Head and Neck Surgery, Aarhus University Hospital, Aarhus, Denmark

² Department of Clinical Medicine, Faculty of Health, Aarhus University, Aarhus, Denmark

³ Department of Oto-Rhino-Laryngology, Head and Neck Surgery, Odense University Hospital, Odense, Denmark

⁴ Department of Endocrinology, Odense University Hospital, Odense, Denmark

recommended for histopathological verification of the diagnosis [3, 12]. A diagnostic challenge applies in particular to patients with FNAB categorized into the heterogeneous group of indeterminate results (BSRTC 3–5) and to those with persistently non-diagnostic (ND, BSRTC 1) samples [12, 14].

The increased detection of thyroid nodules by imaging, combined with the low rate of thyroid nodules harboring malignancy [3], calls for improved preoperative risk-stratification tools to depicting patients with thyroid carcinoma. This would potentially allow a more individualized management, eventually leading to fewer diagnostic thyroid operations.

Elastography

The palpation of tumors for an assessment of tissue stiffness is a fundamental and ancient clinical examination used in clinical practice. Generally, malignant tumors are believed to be stiffer than benign ones, but there are exceptions (e.g., fibrosis or cystic areas). Furthermore, findings by palpation are highly investigator dependent [15]. Ultrasound elastography measures tissue elasticity (stiffness) in a more objective manner, based on an automatic detection of tissue movements induced by externally applied forces [16]. Elastographic methods are categorized according to the external force employed, the measured quantity, and the manner how results are displayed [17]. The multiple ways of categorizing the various technologies have led to terminological inconsistency, and various acronyms may apply to similar methods provided by different manufacturers.

The quasi-static method, termed strain elastography (SE), relies on manually applied pressure on the transducer by the investigator or from carotid artery pulsation to cause tissue deformation [18]. From the registration of tissue deformation (strain), being inversely related to tissue stiffness, a qualitative elasticity map or semi-quantitative ratio of elasticity measurement is displayed [16, 18]. SE was the first elastographic method available for thyroid evaluation. However, strain of a thyroid nodule is influenced by adjacent thyroid tissue and moreover, SE has limitations in the evaluation of multinodular goiter, deeply located nodules, and in nodules containing calcifications [16, 19].

The dynamic methods covering acoustic radiation force impulse (ARFI) imaging, 2D shear wave elastography (SWE), and point SWE (pSWE) apply standardized acoustic impulses from the US transducer to induce minute tissue movements resulting in transverse shear waves. The shear wave speed is then registered and translated into a quantitative measurement of elasticity [16, 18, 19]. These technologies are believed to be less user dependent and, when introduced, considered more technologically advanced compared

with SE [18]. The technologies differ with regard to the size of the measured area, the method for tissue displacement, and their way to display the elasticity signal alongside the quantitative measurements [16].

US elastography constitutes a natural extension of gray-scale US in the evaluation of thyroid nodules. Several studies, employing different methodologies, have shown promising results of elastography in the evaluation of thyroid nodules, with reports of lower elasticity (i.e., higher stiffness) in malignant than in benign thyroid nodules [20–22].

Shear wave elastography

Real-time 2D SWE (hereafter termed SWE) measures real-time tissue elasticity, quantified as an elasticity index (EI) expressed in kilopascal (kPa or m/s), along with a qualitative color-coded elasticity map [16, 23, 24]. The technology exploits the registration of shear waves generated by tiny tissue movements resulting from acoustic impulses emitted from the US transducer along a pushing line [16]. The speed of the shear waves along several simultaneous pushing lines is registered by the US apparatus and is closely related to tissue elasticity, applying Young's modulus [17]. Hereby, a live color-coded elasticity map of 2×3 cm is displayed overlaying the gray-scale US image [16], and with corresponding measurements of elasticity expressed in kPa (Fig. 1). After freezing the elasticity map, the investigator places a movable and size adjustable region of interest (ROI), whereby quantitative EI measurements are displayed (Fig. 1).

SWE is believed to be less user dependent than qualitative or semi-quantitative quasi-static methods, as SWE uses acoustic impulses generated by the transducer to measure elasticity, rather than external pressure applied by the investigator [16, 19]. Further, the technology allows for assessment of the distribution and heterogeneity of elasticity within a large area, both qualitatively and quantitatively, with the possibility of avoiding artifacts during ROI placement. Also, elasticity is quantified by EI, allowing for comparison between adjacent areas (EI ratio) or registration of changes over time. Finally, split-screen mode allows simultaneous assessment of morphology and elasticity, ensuring that EI is measured within the index nodule [16].

A higher EI in thyroid carcinoma compared with benign thyroid nodules has been reported [25–39], and SWE has been proposed as an adjuvant to conventional gray-scale US [24, 29, 30]. However, EI values of malignant and benign nodules overlap, and cut-off points for the differentiation between thyroid carcinoma and benign nodules diverge, ranging from 22 to 94 kPa [25–39].

Thus, the clinical application of SWE is unclear, despite the fact that the first report was published ten years ago [25]. Therefore, we reviewed studies of SWE, with special focus

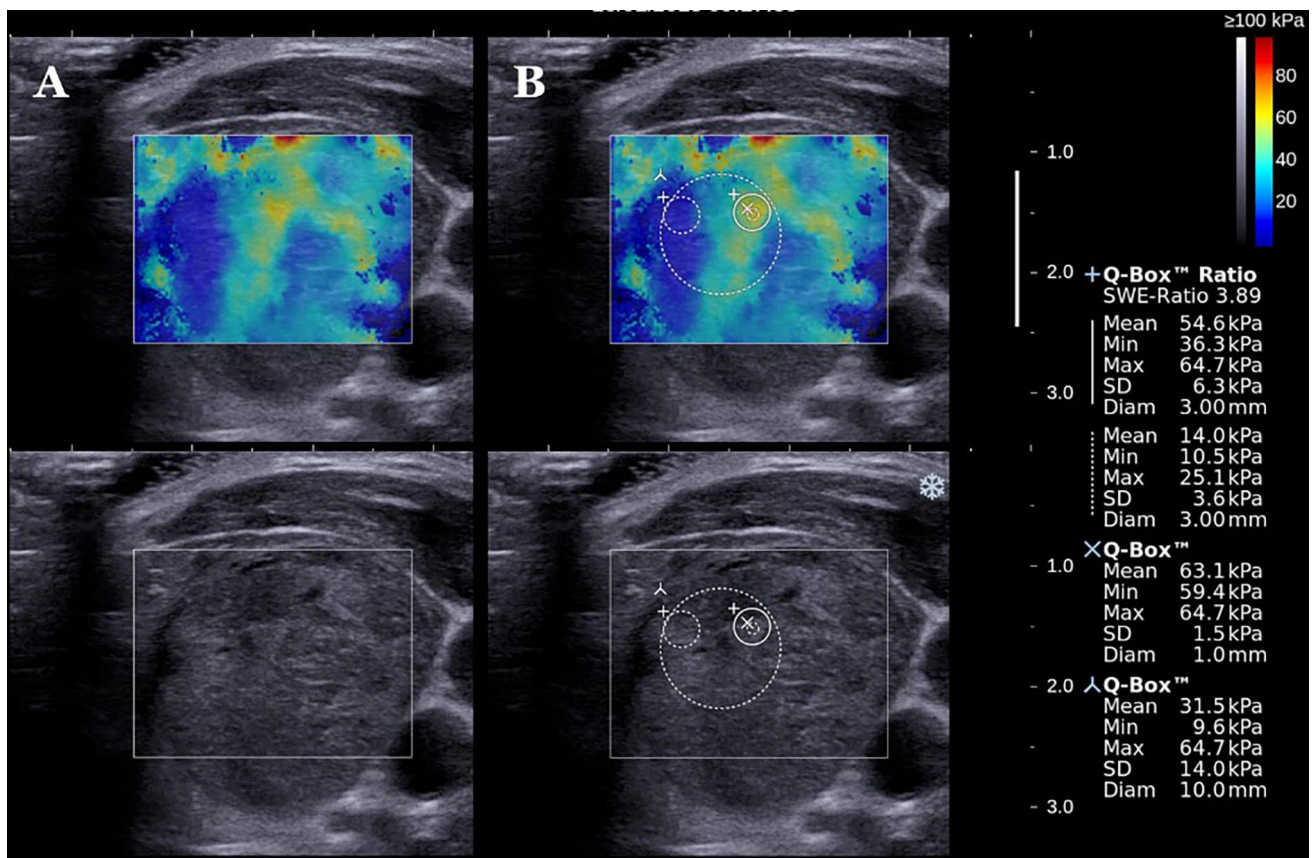


Fig. 1 SWE image depicting the SWE acquisition- and ROI placement process. **a** Frozen SWE image; **b** the same SWE image with ROIs and, to the right, EI measurements

on the clinical applicability, and balancing the advantages and the shortcomings of the method.

Materials and methods

A comprehensive literature search (24th February 2020) was conducted in PubMed using the terms “thyroid” AND “shear wave elastography” or “thyroid” AND “elastography”. Reference lists of screened and included papers were reviewed for additional studies. First, titles were screened, then abstracts, and finally full texts were read by one author (KZS). The flowchart of literature selection is depicted in Fig. 2. The inclusion criteria were: (1) SWE performed in diagnostic studies of thyroid nodules in regard to differentiating malignant from benign nodules or studies of thyroid nodular SWE reproducibility, (2) Quantitative assessment reporting EI measurements, (3) adult patients (≥ 18 years), and (4) English language. The included studies are listed in Tables 1, 2. No meta-analysis assessing diagnostic performance was performed due to large heterogeneity across studies in regard to elasticity measurements and cut-off points.

Results

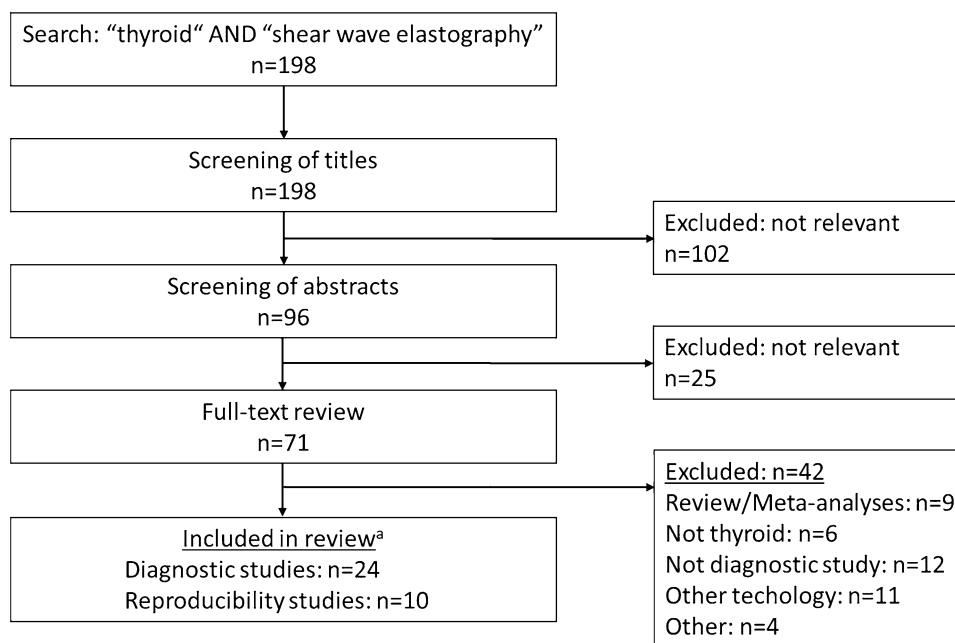
Diagnostic properties of thyroid SWE

Many authors reported higher EI in malignant compared with benign nodules [25–35, 37, 40–46]. During the past few years, less encouraging results have emerged, as two studies reported almost similar EI values for benign and malignant thyroid nodules [47, 48].

Original studies investigating the diagnostic performance of thyroid SWE are summarized in Table 1. Significant heterogeneity exists regarding the optimum parameter for elasticity assessment, definition of ROI for EI measurements, EI cut-off points, elasticity scale settings, and the scanning planes used [18, 49]. Elasticity assessments around the stiffest area of the nodule are the most common EI outcomes reported, reflected by measures of mean and maximum elasticity.

The majority of the proposed EI cut-off points (Table 1) reflect a suboptimal diagnostic accuracy, as determined by the area under the curve (AUC) in ROC analyses. AUC ranged from 0.61 to 0.94, and 89% of the studies show an AUC within the range 0.70–0.90. Specificity and

Fig. 2 Flow-chart of study selection ^a5 studies assess both diagnostic properties and reproducibility of SWE



sensitivity were 0.48–0.97 and 0.42–0.95, respectively, (Table 1). The first report on this particular method found an exceptionally high AUC of 0.94 [25], but subsequent studies failed to reproduce such an encouraging result. Thus, although several studies provide fairly operational EI cut-off levels on a group basis, the diagnostic value in the individual patient is suboptimal, explained by the huge overlap in EI between benign and malignant nodules (Table 1).

Several meta-analyses of the diagnostic accuracy of thyroid SWE have been performed, and with diverging results [20, 21, 49–54]. Although the pooled sensitivity and specificity found in some studies seem encouraging, the clinical utility of these analyses is highly questionable, as various technologies (SWE, pSWE, ARFI) were pooled, patient cohorts were highly heterogeneous, and a range of different cut-off points were used for determining the outcomes. One meta-analysis, including SWE studies only, found suboptimal performance of the method, reflected by a sensitivity and a specificity of 0.66 and 0.78, respectively [51].

Two recent studies evaluated a novel 3D SWE method [38, 41]. 3D SWE uses a similar technology as in 2D SWE, but by inclusion of volume measurements, a three-dimensional EI map is generated with several image slices. This technology might seem promising but the diagnostic accuracy turned out to be similar or even lower than achieved by 2D SWE [38, 41]. Thus, this extended version of SWE seems not to overcome the current limitations of the technology.

Efforts have been made to establish a relevant subgroup of patients, in whom SWE would improve the accuracy of thyroid nodular risk-stratification [26, 31, 36, 37, 47,

48]. However, as such a subgroup remains to be identified, and the risk of misclassifying thyroid nodules is currently unacceptably high, if based only on SWE results.

SWE has been suggested as an add-on investigation to gray-scale US to select patients for FNAB or surgery, rather than a separate diagnostic tool replacing conventional US or even FNAB [22, 24, 29, 30]. The diagnostic accuracy of SWE as an adjuvant examination has been addressed in several studies, but results have been conflicting [25–27, 30, 41, 44, 45, 55]. Although sensitivity may increase when combining US and SWE, as compared with SWE or US alone, a decline in specificity is seen [26, 27, 29, 30, 41]. Some studies reported no change in the diagnostic performance when combining SWE and US compared with SWE alone, whereas other reports were more positive [25, 31, 44, 45]. In a recent study [56], a combination of qualitative assessment of SWE images and a preoperative BRAF gene detection was superior to the individual performance of both tools in terms of identifying cancer. The combined method showed a sensitivity of 93% and a specificity of 95% [56]. Such diagnostic performance seems high but needs to be confirmed in prospective studies.

For the identification of malignant nodules embedded in a multinodular goiter, SWE has shown better performance than indices of nodule size or suspicious US features [57]. SWE may also be employed for prognostication of PTC, as a positive association seems to exist between EI and factors like extra-thyroidal extension, multifocality, and central lymph node metastasis [58].

Table 1 Studies evaluating the diagnostic accuracy of SWE of thyroid nodules

Study	Patients/nodules, <i>n</i> Cancer/PTC, %	EI outcome	Elasticity index, kPa			Cut-off, kPa	Sens	Spec	AUC
			Mean ± SD or Median (range)	Malignant	Benign				
Sebag ^a [25]	93/144 20%/70%	N/A	150 ± 95 (30–356)	36 ± 30 (0–200)	<0.001	65	0.85	0.94	0.94
Bhatia ^a [36]	74 ^b /62 27%/76%	Mean	43 (12–188)	26 (7–132)	NS ^c	42.1	0.53	0.78	0.62
		Max	49 (20–252)	35 (13–163)	NS ^c	82.0	0.35	0.89	0.61
Veyrieres [26]	148/297 12%/80%	Max	112 (0–300)	36 (14–230)	<0.001	66	0.80	0.91	0.85
Kim ^a [27]	99/99 21%/100%	Mean	86 ± 42 (21–166)	52 ± 23 (10–128)	<0.001	62	0.67	0.72	0.77
		Max	100 ± 51 (23–218)	60 ± 28 (17–174)	<0.001	65	0.76	0.64	0.76
Szczepanek-Parulska [28]	122/393 6%/82%	Mean ^d	143 (8–294)	25 (1–181)	<0.0001	49	0.86	0.81	–
		Max ^d	191 (14–300)	35 (1–300)	<0.0001	50	0.95	0.67	–
Liu ^a [29]	271/331 31%/98%	Mean	64 ± 42	28 ± 16	<0.001	39.3	0.66	0.84	0.81
		Max	80 ± 51	38 ± 20	<0.001	43.8	0.69	0.77	0.80
Park ^a [30]	453/476 80%/99%PTC	Mean	88 ± 51	56 ± 26	<0.001	85.2	0.44	0.89	–
		Max	103 ± 62	66 ± 31	<0.001	94.0	0.46	0.86	–
Samir [37]	35/35 ^e 31%/55%	Mean	31 ± 14	18 ± 8	<0.001	22.3	0.82	0.88	0.81
Duan [31] ^f	118/137 66%/100%	Mean	47 ± 17	28 ± 12	0.003	34.5	0.84	0.77	0.79
		Max	74 ± 18	50 ± 23	>0.05	53.2	0.82	0.62	0.70
Chen [33]	253/319 43%/79%	N/A	49 ± 23	18 ± 20	<0.001	27.6	0.85	0.84	0.77
Dobruch-Sobczak ^a [32]	119/169 30%/86%	Mean	54	29	0.0003	30.5	0.64	0.67	–
		Max	88	46	0.0003	67.0	0.42	0.88	–
Wang [40]	185/215 82%/94%	Mean	68 ± 40	46 ± 27	<0.001	45.9	–	–	–
		Max	85 ± 53	61 ± 45	<0.001	65.0	–	–	–
He ^a [34]	140/140 34%/98%	Mean	31 ± 17	20 ± 7	<0.001	–	–	–	0.75
		Max	64 ± 47	34 ± 16	<0.001	42.9	0.64	0.88	0.80
Liu ^a [35]	227/313 62%/98%	Max	64 ± 47	34 ± 16	<0.001	42.9	0.64	0.88	0.80
		Max	73 ± 36	41 ± 15	<0.001	51.9	0.81	0.83	0.88
Bardet [47]	131/131 16%/43%	Mean	20 ± 12	20 ± 15	0.46	–	–	–	–
Kim ^a [39]	105/105 13%/100%	Mean	37 (24–85)	24 (17–32)	0.005	33.3	0.57	0.86	0.74
		Max	47 (35–120)	32 (23–36)	<0.001	45.9	0.57	0.88	0.80
		SD	6.3 (4.1–17.3)	2.6 (1.8–4.1)	<0.001	6.5	0.50	0.97	0.85
Zhao ^a [38]	176/176 36%/94%	Mean	58 ± 30	28 ± 14	<0.001	40.6	0.68	0.88	0.82
		Max	78 ± 39	38 ± 18	<0.001	49.5	0.75	0.82	0.84
Hang [44]	262/298 59%/99%	Max	79 ± 41	50 ± 26	0.001	52.7	–	–	–
Kyriakidou ^a [43]	62/84 13%/82%	Mean	2.9 ± 0.7 m/s	2.5 ± 0.5 m/s	0.03	21.07 kPa	0.73	0.67	0.71
Yang ^a [45]	150/168 54%/84%	Mean	57 ± 27	28 ± 7	<0.05	42.3	–	–	0.86
Swan [48]	329/413 21%/65%	Mean	27 (3–100)	28 (4–182)	0.78	–	–	–	–
		Max	40 (11–148)	39 (6–242)	0.50	–	–	–	–
Han [41]	96/97 61%/92%	Mean	32 ± 17	21 ± 6	<0.001	23.75	0.70	0.76	0.75
		Max	68 ± 52	38 ± 14	<0.001	54.85	0.48	0.90	0.72
Farghadani ^a [42]	57/57 12%/86%	Mean	83 ± 47	44 ± 33	0.01	39.6	0.86	0.66	0.79

Table 1 (continued)

Study	Patients/nodules, <i>n</i> Cancer/PTC, %	EI outcome	Elasticity index, kPa			Cut-off, kPa	Sens	Spec	AUC
			Mean ± SD or Median (range)						
			Malignant	Benign	<i>p</i> value				
Shang [46] ^f	446/510 80%/100%	Mean	50 ± 16	36 ± 13	<0.0001	34.5	0.87	0.52	0.75
		Max	73 ± 28	51 ± 16	<0.0001	64.5	0.57	0.84	0.77

PTC papillary thyroid carcinoma, EI elasticity index, SD standard deviation, sens sensitivity, spec specificity, AUC area under the curve

^aDiagnosis based on both FNAB and histological examination

^bInitial inclusion of 81 nodules in 74 patients, 19 nodules were excluded due to lack of diagnosis

^cStatistically significant difference between PTC (*n* = 13) only and benign nodules

^dROI placement not specified

^eBSRTC 3–4 patients only

^fOnly nodules with diameter ≤ 10 mm were included

Factors influencing diagnostic accuracy

The EI is influenced by the histological properties of the nodule. PTC—the most common type of TC—is characterized by higher EI as compared with benign nodules as well as other thyroid malignancies [36, 47, 59]. Accordingly, studies including a high percentage of PTC reported the highest EI cut-off points [27, 30], while few cases of PTC result in either a low EI cut-off point [37] or no difference between malignant and benign nodules [47, 48] (Table 1). These findings may partly be explained by the presence of fibrosis, found especially in PTC but also in benign tissue such as chronic autoimmune thyroiditis [60]. Thus, two studies employing SWE and ARFI, respectively [59, 61], found a positive correlation between nodular stiffness and the degree of fibrosis in histological thyroid specimens. These findings indicate that fibrosis may explain, at least partly, the overlap in EI seen between malignant and benign lesions.

Indeterminate cytology is more frequently associated with FTC, thus introducing preselection of these less stiff cancers in studies only investigating indeterminate nodules [37, 47]. On the contrary, studies excluding patients with indeterminate cytology without histological confirmation found higher stiffness of the malignant lesions due to a higher percentage of PTC [29–31, 62, 63].

Nodules size is another factor that should be taken into account. Different cut-off points may be applicable, with higher EI in larger nodules [29, 31, 34, 48]. Interestingly, one study found higher diagnostic accuracy of SWE in nodules less than 1 cm compared with larger nodules [55]. For the diagnosis of micro-PTC, relatively low cut-off points (34.5 kPa) were reported in two studies [31, 46].

Comparison of different technologies

One study, evaluating 84 thyroid nodules, compared the diagnostic accuracy of SE, ARFI, and SWE head-to-head

[43]. AUC of ARFI was similar to that of SWE but was higher compared with SE. In contrast, a more recent study found superior performance of SE in comparison with SWE and Thyroid Imaging Reporting and Data System (TIRADS) [55]. Meta-analyses compared the diagnostic properties of SE against the pooled results of different SWE technologies (SWE, pSWE, ARFI). High diagnostic accuracy of both methodologies was found, with summary AUC in the range of 0.83–0.94, and false-positive and -negative rates of 14.6–16.0% and 3.1–5.0%, respectively [20, 49, 54]. Performance was slightly better for SE than the SWE technologies. However, pooling results from different cohorts, SWE technologies and technical settings, as well as different cut-off points, is not particularly meaningful. Thus, the encouraging results found in previous meta-analyses [20, 21, 49, 50, 52–54] are not clinically viable when pooled performance of different SWE technologies are assessed. When restricting a meta-analysis to studies only using SWE, the result is even less impressive [51].

SWE reproducibility

Agreement between repeated measurements is an important factor, influencing the performance of any diagnostic test. Although SWE is considered to be user independent [16, 19], several investigator-dependent steps may affect SWE acquisition and EI measurement by ROI placement. Therefore, the entire process of SWE acquisition, elasticity interpretation, as well as EI measurement need to be taken into account for an assessment of the SWE reproducibility. Several factors are difficult to standardize, e.g., pre-compression, plane selected for EI measurement, timing when freezing the live color-coded film sequence, and interpretation of artifacts. In contrast, a standardized selection and placement of ROI is easier to accomplish through predefined criteria and specific definitions of ROI [62]. Thus, SWE agreement

Table 2 Studies evaluating the SWE reproducibility of thyroid nodules

Study	Nodules, <i>n</i>	SWE process	Agreement
Bhatia [62]	40	Intrater, Interrater ^b Quantitative Process: acquisition and ROIs	Intrater ICC: 0.82–0.85 Intrater COR: 11.3–23.7 kPa
Veyrieres [26] ^a	152	Interrater Quantitative Process: unclear ^c	Interrater ICC: 0.97
Brezak [65]	41	Inter-, intrater Qualitative, quantitative Process: ROIs on stored images	<i>Qualitative:</i> Interrater Kappa: 0.69–0.81 Intrater Kappa: 0.70–0.78 <i>Quantitative</i> Interrater CCC: 0.93 Intrater CCC: 0.97
Anvari [64]	35	Inter-, intrater agreement Quantitative Process: ROIs on stored cine-loops	Interrater ICC: 0.80–0.96 Intrater ICC: 0.86–0.98
Wang [40] ^a	40	Inter-, intrater Quantitative Process: unclear ^c	Interrater ICC: 0.77–0.82 Intrater ICC: 0.77–0.85
Swan [66]	72	Inter-, intrater, day-to-day Quantitative Process: acquisition and ROIs	Interrater LOA: 1.7–3.6 ratio Intrater LOA: 1.8–3.7 ratio Day-to-day LOA: 2.2–2.9 ratio
He [34] ^a	30	Inter-, intrater Quantitative Process: unclear ^c	Interrater ICC: 0.85 Intrater ICC: 0.95
Bardet [47] ^a	131	Interrater (<i>n</i> = 47), Intrater (<i>n</i> = 131) Quantitative Process: acquisition and ROIs	Interrater CV: 0.26 Interrater ICC: 0.68 Intrater CV: 0.23 Intrater ICC: 0.79
Zhao [38] ^a	30	Inter-, intrater Quantitative Process: unclear ^c	Interrater ICC: 0.82–0.84 Intrater ICC: 0.90–0.92
Yoo [59]	29	Interrater (<i>n</i> = 20), intrater (<i>n</i> = 29) Quantitative Process: ROIs on stored images	Interrater CV: 14.9 Interrater ICC: 0.86 Interrater LOA: – 12.9–13.7 kPa Intrater CV: 7.5–7.6 Intrater ICC: 0.96–0.98

ICC Intra-class correlation coefficients (range: 0–1.0; optimal agreement: 1.0), *Kappa* (range: 0–1.0; optimal agreement: 1.0), *COR* coefficient of repeatability (assesses 95% LOA as absolute value; optimal agreement: 0 kPa), *CCC* concordance correlation coefficient (range: 0–1.0; optimal agreement: 1.0); *CV* coefficient of variation (assessed as percentage; optimal agreement: 0%); *LOA* limits of agreement (assessed as ratio or percentage (optimal agreement: 1.0 or 100%) or absolute value (optimal agreement: 0 kPa); *ROI* region of interest

^aReporting both diagnostic and reliability results

^bResults not reported for thyroid lesions alone

^cProcess not thoroughly described, but most likely the whole process was performed, including both acquisition and ROI placement

is influenced by a number of factors that contribute to the overall variability of the method.

The reproducibility of thyroid SWE has been investigated in several studies [26, 34, 38, 40, 47, 59, 62, 64–66], as listed in Table 2. Data were retrieved by retrospective EI measurements from stored film sequences or images, or by assessment of the whole SWE process during both acquisition and EI measurements (ROI placement) (Table 2) [26, 38, 62, 64, 65].

Diverging results have been reported when evaluating the whole SWE acquisition process. One study found suboptimal agreement, with inter-, intra-, and day-to-day limits of agreement (LOA) ratio in the range of 1.7–3.7 and proportion of agreement in the range 0.63–0.88 [66]. Other studies reported inter-rater intra-class correlation coefficients (ICCs) of 0.34–0.85 and intra-rater ICCs of 0.59–0.85, depending on EI outcomes and heterogeneity of the elasticity map [34, 40, 47, 62]. For further details, see Table 2.

Factors influencing reproducibility

Lower agreement seems to exist when evaluating malignant compared with benign nodules, possibly due to a higher degree of elastic heterogeneity in malignant nodules, especially PTC (Fig. 3) [59, 62, 66].

When only assessing ROI placement rather than the entire SWE acquisition process, studies of the thyroid gland and mammary tissue showed higher agreement, indicating that the largest variation lies within the multiple steps of SWE acquisition [62, 64, 65, 67–69]. One study reported significantly higher agreement by assessing the whole nodule EI, as compared with a 3 mm ROI (defined by the operator) around the stiffest area of the nodule [59]. This observation supports that the SWE acquisition process should be as simple as possible, limiting the number of investigator-dependent steps. Two studies found no influence of investigator experience on the prevalence of artifacts, or on the inter-observer agreement [66, 70].

Estimation of agreement is influenced by the statistical methods applied and the heterogeneity of data, making a comparison across studies difficult [71, 72]. A statistical test using limits of agreement (LOA) is considered the most suitable for a dataset with high heterogeneity. Indeed, heterogeneity of data obtained from thyroid elastography is caused by the inherent feature of the thyroid tissue, as well as variations within and between observers, and from day-to-day [61, 71–73].

Considerations concerning reproducibility

SWE reproducibility is put into further perspective, as it may be affected by the spatial heterogeneity of thyroid morphology [61, 73] as well as the dynamic properties of US [74, 75]. Conventional gray-scale US harbors an inherent inter-observer variability, which most likely influences the acquisition process of elastography. Several studies, investigating observer-agreement of single US features as well as US risk-stratification systems, reported diverging results, ranging from poor to substantial agreement (kappa: 0.11–0.91) [76–81]. Identification of thyroid calcifications has shown high inter-rater agreement (0.67–0.91) [76–78], but depends on the experience of the operator. On the contrary, US features difficult to interpret are nodule borders, the significance of a solid component within a complex nodule, signs of extra-thyroidal growth, and intra-nodular flow assessed by Doppler [10, 76–78]. Inter-observer agreement for US risk-stratification systems (e.g., TIRADS) are generally reported to have higher agreement (0.25–0.76) than single US features [78–81]. The clinical decision-making of when to perform FNAB according to the various US systems showed even higher agreement between investigators [78, 81].

Conflicting results were reported also for reliability assessment of other elastographic technologies applied to the thyroid. For SE, Park et al. [82] found no statistical significant inter-observer correlation for real-time acquisition and the interpretation of elastographic findings, while two

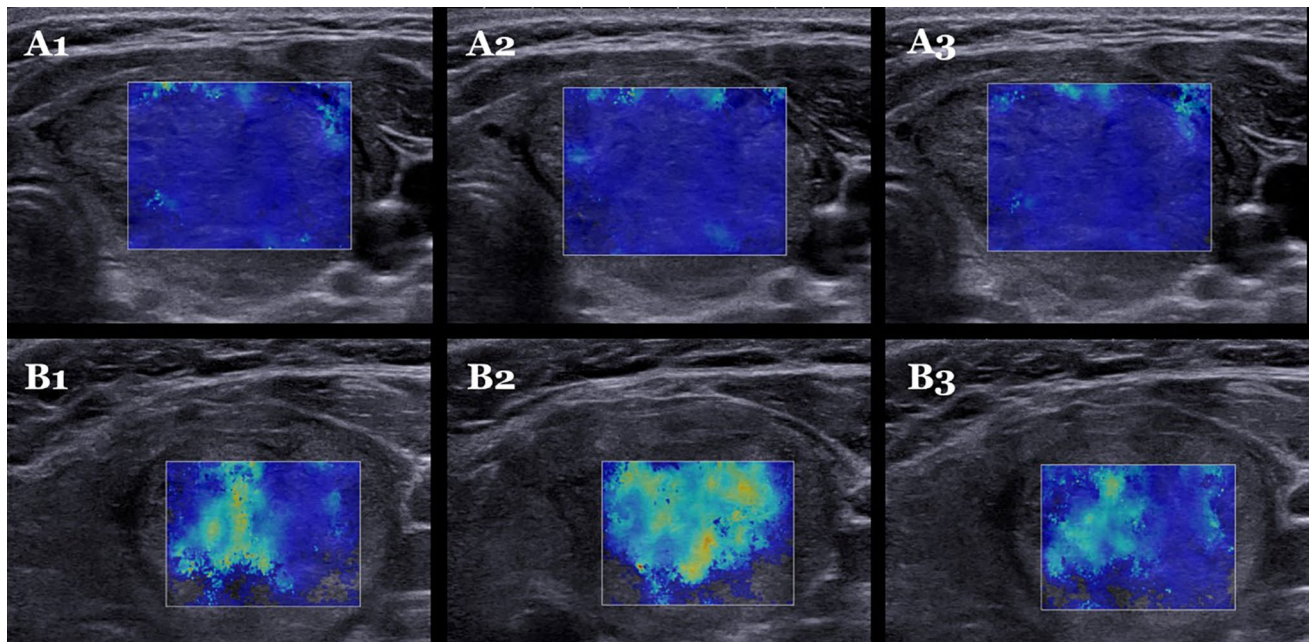


Fig. 3 SWE agreement in elastic homogeneous and heterogeneous nodules. **a1-a3** three consecutive SWE examinations in the same homogeneous nodule. **b1-b3** three consecutive SWE examinations in the same heterogeneous nodule

other studies showed more promising results (inter-rater Cohens' Kappa: 0.64 [83]; 0.74 [63]). Similar levels of reliability apply to ARFI and pSWE [84–86]. In an early SE reliability study [82], assessment of the influence from pre-compression was not possible (pressure control). However, this was implemented in subsequent studies [83], which might explain, in part, the differences across studies in the reliability of this method [22]. Although SE uses manual compression as external force, this technology is not necessarily more operator-dependent than SWE [18].

Methodological issues of thyroid SWE

SWE artifacts

Artifacts may arise during SWE acquisition [70], and caution must be taken when interpreting the elasticity map and the EI measurements (Fig. 4). One study found artifacts in 70% of 1297 SWE images, with the majority (35%) being caused by pre-compression [70]. In 19% of investigated nodules, SWE was uninterpretable due to artifacts. Pre-compression during SWE acquisition results from the pressure

on the transducer applied by the investigator (Fig. 4a). The magnitude of pressure affects tissue elasticity, and EI increases with increasing pre-compression, potentially inducing unintended measurement variability [17, 87, 88]. Nodules located in the isthmus may be more prone to pre-compression due to the proximity to the trachea [18]. Currently, quantification of pre-compression is not possible in SWE; therefore, the use of generous amounts of gel to avoid artifacts at the cervical fascia is recommended.

Artifacts of increased stiffness also occur when structural interfaces are encountered, as disruption of the linear relationship between the speed of the shear waves and the elastic modulus is induced when crossing tissue borders (Fig. 4b). The split-screen mode is helpful in identifying the morphological borders on the gray-scale US, which may not be possible from the elasticity map [16, 17]. Vertical artifacts represent bands of increased stiffness crossing anatomical borders (Fig. 4c) [36]. Movement artifacts during SWE acquisition may arise from tiny unwanted movements of the transducer or the chest due to respiration, which result in persistent color changes in the image beyond the first 3–5 s. Movement artifacts from the carotids are reduced by placing the probe in the longitudinal plane during SWE acquisition

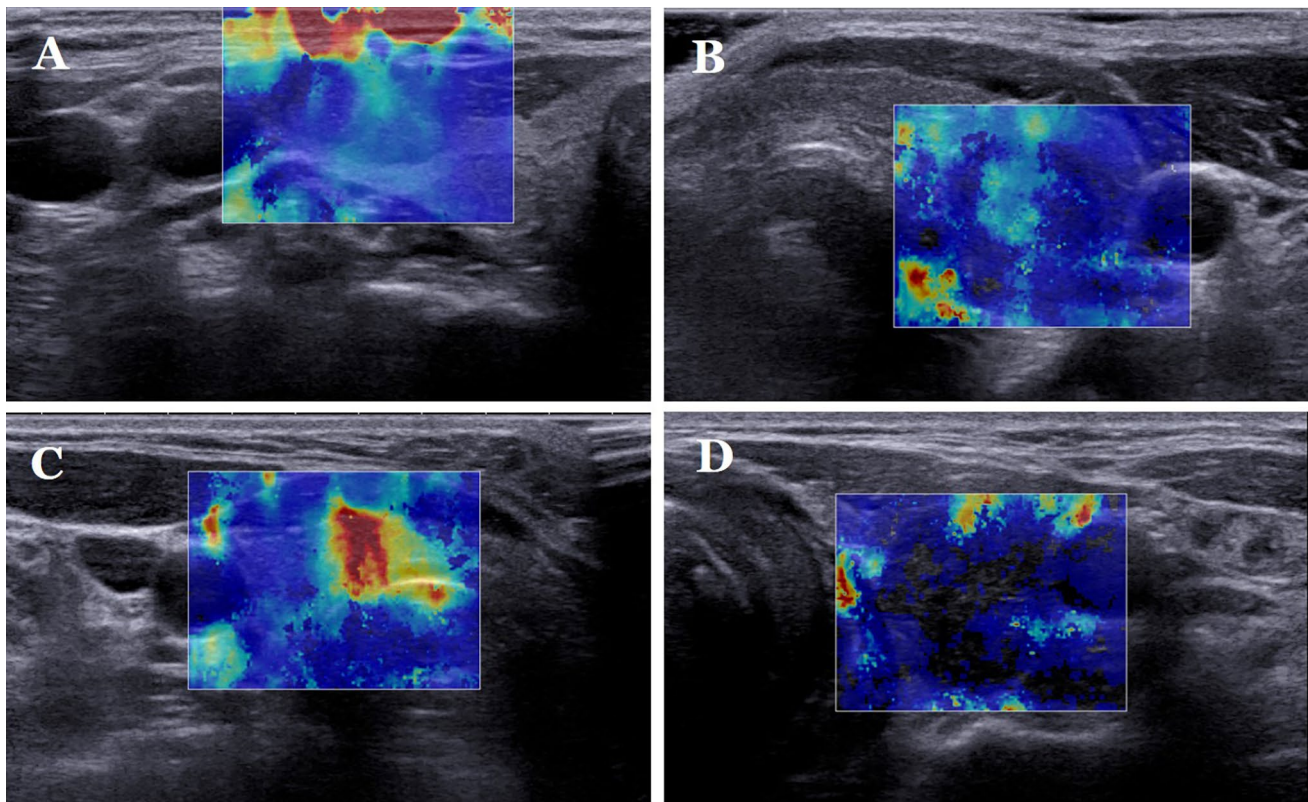


Fig. 4 SWE artifacts. **a** Pre-compression artifact seen by the presence of increased stiffness at the skin surface (red color band at the cervical fascia); **b** Artifact of increased stiffness in tracheal lumen in

proximity to the tracheal cartilage; **c** Increased stiffness within normal thyroid parenchyma medially to a thyroid nodule and anterior to trachea; **d** Poor SWE signal in a marked hypoechoic nodule

[24]. The color codes should be stable before freezing the film sequence prior to EI measurements. However, this may not be possible in heterogeneous nodules, even when no movement is visible, which probably has an unfavorable impact on the EI reproducibility.

Micro- or macrocalcifications may induce increased stiffness [89], and elasticity measures should be avoided in areas with macrocalcifications. Avoiding microcalcifications may be more difficult, and their presence must be taken into account when interpreting EI measurement in nodules harboring such elements [89]. The gray-scale split screen allows the investigator to evaluate whether EI is influenced by calcifications or if other hyperechoic spots are present [10]. Shear waves do not propagate in fluid, making elasticity assessments impossible in cystic areas [16]. In fact, EI may be increased in nodules with cystic areas due to the low deformation potential of fluids [89]. Very hypoechoic or deeply located nodules may reflect a poor or even no SWE signal (Fig. 4d). In these nodules, SWE does not provide reliable information, even when adjusting the settings of the equipment [24, 36]. Poor SWE signal has been associated with malignancy [48], and may, thus, represent a surrogate marker of hypoechogenicity.

Thyroid heterogeneity

Elastography determines tissue elasticity indirectly by measurements of tissue response to applied external stress. The technology behind elastography relies on the assumption that the investigated tissue exhibits simple behavior, such as being linear and homogeneous [16, 90]. However, biological soft tissue exhibits properties of heterogeneity, non-linearity, and viscoelasticity, which makes it less suitable to fit into this simplified model [16, 73]. Although elastography may detect disorders of various organs [25, 26, 28–30, 36, 91–93], interpretation of elasticity data should be done with caution. Artifacts arising during SWE acquisition are largely explained by properties related to soft tissue. Pre-compression artifacts and the increased stiffness with increasing pre-compression load, reported by Lam et al. [87], are explained by the non-linear properties of soft thyroid tissue. Similarly, the heterogeneity of soft tissue, including boundaries between adjacent tissues with different properties, explains the phenomenon of structure interface artifacts [17]. Therefore, when assessing thyroid nodular stiffness, it is important to take into account the heterogeneous nature of thyroid nodules caused by cell density, calcifications, fibrosis, adipose tissue, and cystic areas [61]. These factors apply especially to PTC and may be presented as heterogeneous elasticity maps [73]. Considerable heterogeneity, both within and between subjects, has been reported when assessing the qualitative elasticity map [48, 66]. The standard deviation of EI has recently been proposed as a better measure of

elastic heterogeneity than absolute EI values [39, 46, 48]. However, quantifying this heterogeneity is challenging, and identification of relevant quantitative markers of EI heterogeneity in the prediction of thyroid malignancy is yet to be accomplished and validated [39, 48, 66]. Texture analysis employing mathematical models has also been introduced as a novel method to assess elastic heterogeneity [73]. One feasibility study reported superior performance of texture analysis compared with conventional EI measurements [73]. Although the method seems promising, these findings need to be validated in future studies.

Conclusions

The present SWE technology seems not robust enough to be clinically implemented on a wide scale. SWE may be promising on a group level, but the risk of misclassifying a thyroid nodule seems unacceptably high in the individual patient due to the substantial overlap of EI values observed in benign and malignant lesions. A number of confounding factors affect elasticity measurements such as the heterogeneous nature of thyroid nodules, and the co-existence of fibrosis or autoimmune thyroiditis [60, 61].

In light of current evidence, there is a need for standardization and consensus on the most optimum SWE acquisition process. Operator dependent factors include the applied pre-compression level, the scanning plane, timing when freezing the live SWE film sequence, and the optimum ROIs. One recent guideline [24] suggested such standardization, but it remains to be confirmed in future studies whether this could help identifying a cut-off point that reliably can differentiate malignant from benign thyroid nodules on the individual level. Previous studies were highly heterogeneous in regard to the risk of malignancy, the process of SWE acquisition, as well as the EI endpoints evaluated, factors that hinder a reliable meta-analysis to be performed. The low observer agreement and the diverging results of repeated measurements add further concern to the clinical applicability of the current SWE method. This is probably explained by methodological limitations of the technology per se, in combination with the high degree of heterogeneity of thyroid nodular tissue [22]. Thus, it remains to be demonstrated whether clinically useful information can be achieved in patients with thyroid nodules, when SWE is applied on top of other US characteristics or genetic testing.

Author contributions All authors contributed significantly to the work. The literature search and selection as well as data extraction was performed by KZS. The primary author of the manuscript draft and revisions is KZS. VEN and SJB contributed by revision of the manuscript and supervision throughout the process.

Funding Fonden af 17-12-1981 and Aarhus University (KZS fellowship).

Declarations

Conflict of interest On behalf of all authors, the corresponding author states that there is no conflict of interest.

Ethical approval This article does not contain any studies with human participants or animals performed by any of the authors.

References

- Hegedus L, Bonnema SJ, Bennedbaek FN (2003) Management of simple nodular goiter: current status and future perspectives. *Endocr Rev* 24(1):102–132. <https://doi.org/10.1210/er.2002-0016>
- Hegedus L (2004) Clinical practice. The thyroid nodule. *N Engl J Med* 351(17):1764–1771
- Haugen BR, Alexander EK, Bible KC, Doherty GM, Mandel SJ, Nikiforov YE et al (2016) 2015 American Thyroid Association management guidelines for adult patients with thyroid nodules and differentiated thyroid cancer: The American Thyroid Association guidelines task force on thyroid nodules and differentiated thyroid cancer. *Thyroid* 26(1):1–133. <https://doi.org/10.1089/thy.2015.0020>
- Sherman SI (2003) Thyroid carcinoma. *Lancet* 361(9356):501–511
- Gilliland FD, Hunt WC, Morris DM, Key CR (1997) Prognostic factors for thyroid carcinoma. A population-based study of 15,698 cases from the Surveillance, Epidemiology and End Results (SEER) program 1973–1991. *Cancer* 79(3):564–573
- Xing M, Haugen BR, Schlumberger M (2013) Progress in molecular-based management of differentiated thyroid cancer. *Lancet* 381(9871):1058–1069. [https://doi.org/10.1016/S0140-6736\(13\)60109-9](https://doi.org/10.1016/S0140-6736(13)60109-9)
- Mazzaferrri EL, Jhiang SM (1994) Long-term impact of initial surgical and medical therapy on papillary and follicular thyroid cancer. *Am J Med* 97(5):418–428
- Magarey MJ, Freeman JL (2013) Recurrent well-differentiated thyroid carcinoma. *Oral Oncol* 49(7):689–694. <https://doi.org/10.1016/j.oraloncology.2013.03.434>
- Hollenbeak CS, Boltz MM, Schaefer EW, Saunders BD, Goldenberg D (2013) Recurrence of differentiated thyroid cancer in the elderly. *Eur J Endocrinol* 168(4):549–556. <https://doi.org/10.1530/EJE-12-0848>
- Russ G, Bonnema SJ, Erdogan MF, Durante C, Ngu R, Leenhardt L et al (2017) European Thyroid Association guidelines for ultrasound malignancy risk stratification of thyroid nodules in adults: the EU-TIRADS. *Eur Thyroid J* 6(5):225–237
- Nygaard B, Knudsen N, Bennedbaek F, Ebbenhøj E, Sigurd L, Pedersen IB (2020) NBV: Knuden i thyroidea. www.endocrinology.dk
- Cibas ES, Ali SZ (2017) The 2017 Bethesda system for reporting thyroid cytopathology. *Thyroid* 27(11):1341–1346. <https://doi.org/10.1089/thy.2017.0500>
- Cibas ES, Ali SZ (2009) The Bethesda system for reporting thyroid cytopathology. *Am J Clin Pathol* 132(5):658–665
- Bose S, Walts AE (2012) Thyroid fine needle aspirate: a post-Bethesda update. *Adv Anat Pathol* 19(3):160–169. <https://doi.org/10.1097/PAP.0b013e3182534610>
- Jarlov AE, Hegedus L, Gjørup T, Hansen JM (1991) Observer variation in the clinical assessment of the thyroid gland. *J Intern Med* 229(2):159–161
- Bamber J, Cosgrove D, Dietrich CF, Fromageau J, Bojunga J, Calliada F et al (2013) EFSUMB guidelines and recommendations on the clinical use of ultrasound elastography. Part 1: basic principles and technology. *Ultraschall Med* 34(2):169–184
- Shiina T, Nightingale KR, Palmeri ML, Hall TJ, Bamber JC, Barr RG et al (2015) WFUMB guidelines and recommendations for clinical use of ultrasound elastography: Part 1: basic principles and terminology. *Ultrasound Med Biol* 41(5):1126–1147. <https://doi.org/10.1016/j.ultrasmedbio.2015.03.009>
- Monpeyssen H, Tramalloni J, Poiree S, Helenon O, Correas JM (2013) Elastography of the thyroid. *Diagn Interv Imaging* 94(5):535–544. <https://doi.org/10.1016/j.diii.2013.01.023>
- Cosgrove D, Piscaglia F, Bamber J, Bojunga J, Correas JM, Gilja OH et al (2013) EFSUMB guidelines and recommendations on the clinical use of ultrasound elastography. Part 2: clinical applications. *Ultraschall Med* 34(3):238–253
- Tian W, Hao S, Gao B, Jiang Y, Zhang S, Guo L et al (2015) Comparison of diagnostic accuracy of real-time elastography and shear wave elastography in differentiation malignant from benign thyroid nodules. *Medicine (Baltimore)* 94(52):e2312. <https://doi.org/10.1097/MD.0000000000002312>
- Lin P, Chen M, Liu B, Wang S, Li X (2014) Diagnostic performance of shear wave elastography in the identification of malignant thyroid nodules: a meta-analysis. *Eur Radiol* 24(11):2729–2738. <https://doi.org/10.1007/s00330-014-3320-9>
- Cosgrove D, Barr R, Bojunga J, Cantisani V, Chammas MC, Dighe M et al (2017) WFUMB guidelines and recommendations on the clinical use of ultrasound elastography: Part 4. Thyroid. *Ultrasound Med Biol* 43(1):4–26. <https://doi.org/10.1016/j.ultrasmedbio.2016.06.022>
- Zhao CK, Xu HX (2019) Ultrasound elastography of the thyroid: principles and current status. *Ultrasonography* 38(2):106–124. <https://doi.org/10.14366/usg.18037>
- Xu HX, Yan K, Liu BJ, Liu WY, Tang LN, Zhou Q et al (2019) Guidelines and recommendations on the clinical use of shear wave elastography for evaluating thyroid nodule 1. *Clin Hemorheol Microcirc* 72(1):39–60. <https://doi.org/10.3233/CH-180452>
- Sebag F, Vaillant-Lombard J, Berbis J, Griset V, Henry JF, Petit P et al (2010) Shear wave elastography: a new ultrasound imaging mode for the differential diagnosis of benign and malignant thyroid nodules. *J Clin Endocrinol Metab* 95(12):5281–5288
- Veyrieres JB, Albarel F, Lombard JV, Berbis J, Sebag F, Oliver C et al (2012) A threshold value in Shear Wave elastography to rule out malignant thyroid nodules: a reality? *Eur J Radiol* 81(12):3965–3972
- Kim H, Kim JA, Son EJ, Youk JH (2013) Quantitative assessment of shear-wave ultrasound elastography in thyroid nodules: diagnostic performance for predicting malignancy. *Eur Radiol* 23(9):2532–2537
- Szczepanek-Parulska E, Wolinski K, Stangierski A, Gurgul E, Biczysko M, Majewski P et al (2013) Comparison of diagnostic value of conventional ultrasonography and shear wave elastography in the prediction of thyroid lesions malignancy. *PLoS ONE* 8(11):e81532. <https://doi.org/10.1371/journal.pone.0081532>
- Liu B, Liang J, Zheng Y, Xie X, Huang G, Zhou L et al (2015) Two-dimensional shear wave elastography as promising diagnostic tool for predicting malignant thyroid nodules: a prospective single-centre experience. *Eur Radiol* 25(3):624–634. <https://doi.org/10.1007/s00330-014-3455-8>
- Park AY, Son EJ, Han K, Youk JH, Kim JA, Park CS (2015) Shear wave elastography of thyroid nodules for the prediction of malignancy in a large scale study. *Eur J Radiol* 84(3):407–412. <https://doi.org/10.1016/j.ejrad.2014.11.019>
- Duan SB, Yu J, Li X, Han ZY, Zhai HY, Liang P (2016) Diagnostic value of two-dimensional shear wave elastography in

- papillary thyroid microcarcinoma. *Onco Targets Ther* 9:1311–1317. <https://doi.org/10.2147/OTT.S98583>
32. Dobruch-Sobczak K, Zalewska EB, Guminska A, Slapa RZ, Mlosek K, Wareluk P et al (2016) Diagnostic performance of shear wave elastography parameters alone and in combination with conventional B-mode ultrasound parameters for the characterization of thyroid nodules: a prospective, dual-center study. *Ultrasound Med Biol* 42(12):2803–2811. <https://doi.org/10.1016/j.ultrasmedbio.2016.07.010>
 33. Chen M, Zhang KQ, Xu YF, Zhang SM, Cao Y, Sun WQ (2016) Shear wave elastography and contrast-enhanced ultrasonography in the diagnosis of thyroid malignant nodules. *Mol Clin Oncol* 5(6):724–730. <https://doi.org/10.3892/mco.2016.1053>
 34. He YP, Xu HX, Wang D, Li XL, Ren WW, Zhao CK et al (2017) First experience of comparisons between two different shear wave speed imaging systems in differentiating malignant from benign thyroid nodules. *Clin Hemorheol Microcirc* 65(4):349–361. <https://doi.org/10.3233/CH-16197>
 35. Liu Z, Jing H, Han X, Shao H, Sun YX, Wang QC et al (2017) Shear wave elastography combined with the thyroid imaging reporting and data system for malignancy risk stratification in thyroid nodules. *Oncotarget* 8(26):43406–43416. <https://doi.org/10.18632/oncotarget.15018>
 36. Bhatia KS, Tong CS, Cho CC, Yuen EH, Lee YY, Ahuja AT (2012) Shear wave elastography of thyroid nodules in routine clinical practice: preliminary observations and utility for detecting malignancy. *Eur Radiol* 22(11):2397–2406
 37. Samir AE, Dhyani M, Anvari A, Prescott J, Halpern EF, Faquin WC et al (2015) Shear-wave elastography for the preoperative risk stratification of follicular-patterned lesions of the thyroid: diagnostic accuracy and optimal measurement plane. *Radiology* 277(2):565–573. <https://doi.org/10.1148/radiol.2015141627>
 38. Zhao CK, Chen SG, Alizad A, He YP, Wang Q, Wang D et al (2018) Three-dimensional shear wave elastography for differentiating benign from malignant thyroid nodules. *J Ultrasound Med*. <https://doi.org/10.1002/jum.14531>
 39. Kim HJ, Kwak MK, Choi IH, Jin SY, Park HK, Byun DW et al (2018) Utility of shear wave elastography to detect papillary thyroid carcinoma in thyroid nodules: efficacy of the standard deviation elasticity. *Korean J Intern Med*. <https://doi.org/10.3904/kjim.2016.326>
 40. Wang F, Chang C, Gao Y, Chen YL, Chen M, Feng LQ (2016) Does shear wave elastography provide additional value in the evaluation of thyroid nodules that are suspicious for malignancy? *J Ultrasound Med* 35(11):2397–2404. <https://doi.org/10.7863/ultra.15.09009>
 41. Han RJ, Du J, Li FH, Zong HR, Wang JD, Shen YL et al (2019) Comparisons and combined application of two-dimensional and three-dimensional real-time shear wave elastography in diagnosis of thyroid nodules. *J Cancer* 10(9):1975–1984. <https://doi.org/10.7150/jca.30135>
 42. Farghadani M, Tabatabaei SA, Barikbin R, Shahsanai A, Ria-hinezhad M, Jafarpishe S (2019) Comparing the sensitivity and specificity of two-dimensional shear wave elastography and fine needle aspiration in determining malignant thyroid nodules. *Adv Biomed Res* 8:30. https://doi.org/10.4103/abr.abr_215_18
 43. Kyriakidou G, Friedrich-Rust M, Bon D, Sircar I, Schrecker C, Bogdanou D et al (2018) Comparison of strain elastography, point shear wave elastography using acoustic radiation force impulse imaging and 2D-shear wave elastography for the differentiation of thyroid nodules. *PLoS ONE* 13(9):e0204095. <https://doi.org/10.1371/journal.pone.0204095>
 44. Hang J, Li F, Qiao XH, Ye XH, Li A, Du LF (2018) Combination of maximum shear wave elasticity modulus and TIRADS improves the diagnostic specificity in characterizing thyroid nodules: a retrospective study. *Int J Endocrinol* 2018:4923050. <https://doi.org/10.1155/2018/4923050>
 45. Yang JR, Song Y, Xue SS, Ruan LT (2019) Suggested amendment of TI-RADS classification of thyroid nodules by shear wave elastography. *Acta Radiol*. <https://doi.org/10.1177/0284185119889567>
 46. Shang H, Wu B, Liu Z, Liu Y, Cheng W (2020) The effectiveness of shear wave elastography in the diagnosis of PTMC. *Technol Health Care* 28(2):221–226. <https://doi.org/10.3233/THC-191895>
 47. Bardet S, Ciappuccini R, Pellot-Barakat C, Monpeyssen H, Michels JJ, Tissier F et al (2017) Shear wave elastography in thyroid nodules with indeterminate cytology: results of a prospective bicentric study. *Thyroid* 27(11):1441–1449. <https://doi.org/10.1089/thy.2017.0293>
 48. Swan KZ, Bonnema SJ, Jespersen ML, Nielsen VE (2019) Reappraisal of shear wave elastography as a diagnostic tool for identifying thyroid carcinoma. *Endocr Connect* 8(8):1195–1205. <https://doi.org/10.1530/EC-19-0324>
 49. Tian W, Hao S, Gao B, Jiang Y, Zhang X, Zhang S et al (2016) Comparing the diagnostic accuracy of RTE and SWE in differentiating malignant thyroid nodules from benign ones: a meta-analysis. *Cell Physiol Biochem* 39(6):2451–2463. <https://doi.org/10.1159/000452513>
 50. Zhang B, Ma X, Wu N, Liu L, Liu X, Zhang J et al (2013) Shear wave elastography for differentiation of benign and malignant thyroid nodules: a meta-analysis. *J Ultrasound Med* 32(12):2163–2169. <https://doi.org/10.7863/ultra.32.12.2163>
 51. Nattabi HA, Sharif NM, Yahya N, Ahmad R, Mohamad M, Zaki FM et al (2017) Is diagnostic performance of quantitative 2D-shear wave elastography optimal for clinical classification of benign and malignant thyroid nodules?: A systematic review and meta-analysis. *Acad Radiol*. <https://doi.org/10.1016/j.acra.2017.09.002>
 52. Chang N, Zhang X, Wan W, Zhang C, Zhang X (2018) The preciseness in diagnosing thyroid malignant nodules using shear wave elastography. *Med Sci Monit* 24:671–677
 53. Huang R, Jiang L, Xu Y, Gong Y, Ran H, Wang Z et al (2019) Comparative diagnostic accuracy of contrast-enhanced ultrasound and shear wave elastography in differentiating benign and malignant lesions: a network meta-analysis. *Front Oncol* 9:102. <https://doi.org/10.3389/fonc.2019.00102>
 54. Hu X, Liu Y, Qian L (2017) Diagnostic potential of real-time elastography (RTE) and shear wave elastography (SWE) to differentiate benign and malignant thyroid nodules: a systematic review and meta-analysis. *Medicine (Baltimore)* 96(43):e8282. <https://doi.org/10.1097/MD.0000000000008282>
 55. Cantisani V, David E, Grazhdani H, Rubini A, Radzina M, Dietrich CF et al (2019) Prospective evaluation of semiquantitative strain ratio and quantitative 2d ultrasound shear wave elastography (SWE) in association with TIRADS classification for thyroid nodule characterization. *Ultraschall Med* 40(4):495–503. <https://doi.org/10.1055/a-0853-1821>
 56. Wang Y, Wu X, Li J, Chen J, Tan H, Sun L et al (2020) Diagnostic performance of combination of ultrasound elastography and BRAF gene detection in malignant thyroid nodule: a retrospective study. *Int J Clin Exp Pathol* 13(12):2962–2972
 57. Wolinski K, Szczepanek-Parulska E, Stangierski A, Gurgul E, Rewaj-Losyk M, Ruchala M (2014) How to select nodules for fine-needle aspiration biopsy in multinodular goitre. Role of conventional ultrasonography and shear wave elastography—a preliminary study. *Endokrynol Pol* 65(2):114–118. <https://doi.org/10.5603/EP.2014.0016>
 58. Park YJ, Kim JA, Son EJ, Youk JH, Park CS (2013) Quantitative shear wave elastography as a prognostic implication of papillary thyroid carcinoma (PTC): elasticity index can predict extrathyroidal extension (ETE). *Ann Surg Oncol* 20(8):2765–2771

59. Yoo MH, Kim HJ, Choi IH, Park S, Kim SJ, Park HK et al (2020) Shear wave elasticity by tracing total nodule showed high reproducibility and concordance with fibrosis in thyroid cancer. *BMC Cancer* 20(1):118. <https://doi.org/10.1186/s12885-019-6437-z>
60. Magri F, Chytiris S, Capelli V, Alessi S, Nalon E, Rotondi M et al (2012) Shear wave elastography in the diagnosis of thyroid nodules: feasibility in the case of coexistent chronic autoimmune Hashimoto's thyroiditis. *Clin Endocrinol (Oxf)* 76(1):137–141
61. Fukuhara T, Matsuda E, Endo Y, Takenobu M, Izawa S, Fujiwara K et al (2015) Correlation between quantitative shear wave elastography and pathologic structures of thyroid lesions. *Ultrasound Med Biol* 41(9):2326–2332. <https://doi.org/10.1016/j.ultrasmedbio.2015.05.001>
62. Bhatia K, Tong CS, Cho CC, Yuen EH, Lee J, Ahuja AT (2012) Reliability of shear wave ultrasound elastography for neck lesions identified in routine clinical practice. *Ultraschall Med* 33(5):463–468. <https://doi.org/10.1055/s-0032-1325330>
63. Kim JK, Baek JH, Lee JH, Kim JL, Ha EJ, Kim TY et al (2012) Ultrasound elastography for thyroid nodules: a reliable study? *Ultrasound Med Biol* 38(9):1508–1513. <https://doi.org/10.1016/j.ultrasmedbio.2012.05.017>
64. Anvari A, Dhyani M, Stephen AE, Samir AE (2016) Reliability of shear-wave elastography estimates of the young modulus of tissue in follicular thyroid neoplasms. *AJR Am J Roentgenol* 206(3):609–616. <https://doi.org/10.2214/AJR.15.14676>
65. Brezak R, Hippe D, Thiel J, Dighe MK (2015) Variability in stiffness assessment in a thyroid nodule using shear wave imaging. *Ultrasound Q* 31(4):243–249. <https://doi.org/10.1097/RUQ.0000000000000205>
66. Swan KZ, Nielsen VE, Bibby BM, Bonnema SJ (2017) Is the reproducibility of shear wave elastography of thyroid nodules high enough for clinical use? A methodological study. *Clin Endocrinol (Oxf)* 86(4):606–613. <https://doi.org/10.1111/cen.13295>
67. Park HY, Han KH, Yoon JH, Moon HJ, Kim MJ, Kim EK (2014) Intra-observer reproducibility and diagnostic performance of breast shear-wave elastography in Asian women. *Ultrasound Med Biol* 40(6):1058–1064. <https://doi.org/10.1016/j.ultrasmedbio.2013.12.021>
68. Cosgrove DO, Berg WA, Dore CJ, Skyba DM, Henry JP, Gay J et al (2012) Shear wave elastography for breast masses is highly reproducible. *Eur Radiol* 22(5):1023–1032. <https://doi.org/10.1007/s00330-011-2340-y>
69. Evans A, Whelehan P, Thomson K, McLean D, Brauer K, Purdie C et al (2010) Quantitative shear wave ultrasound elastography: initial experience in solid breast masses. *Breast Cancer Res* 12(6):R104. <https://doi.org/10.1186/bcr2787>
70. Dighe M, Hippe DS, Thiel J (2018) Artifacts in shear wave elastography images of thyroid nodules. *Ultrasound Med Biol* 44(6):1170–1176. <https://doi.org/10.1016/j.ultrasmedbio.2018.02.007>
71. Kottner J, Audige L, Brorson S, Donner A, Gajewski BJ, Hrobjartsson A et al (2011) Guidelines for reporting reliability and agreement studies (GRRAS) were proposed. *Int J Nurs Stud* 48(6):661–671. <https://doi.org/10.1016/j.ijnurstu.2011.01.016>
72. Bland JM, Altman DG (1990) A note on the use of the intraclass correlation coefficient in the evaluation of agreement between two methods of measurement. *Comput Biol Med* 20(5):337–340
73. Bhatia KS, Lam AC, Pang SW, Wang D, Ahuja AT (2016) Feasibility study of texture analysis using ultrasound shear wave elastography to predict malignancy in thyroid nodules. *Ultrasound Med Biol* 42(7):1671–1680. <https://doi.org/10.1016/j.ultrasmedbio.2016.01.013>
74. Ha EJ, Baek JH, Na DG (2017) Risk stratification of thyroid nodules on ultrasonography: current status and perspectives. *Thyroid* 27(12):1463–1468. <https://doi.org/10.1089/thy.2016.0654>
75. Brito JP, Gionfriddo MR, Al Nofal A, Boehmer KR, Leppin AL, Reading C et al (2014) The accuracy of thyroid nodule ultrasound to predict thyroid cancer: systematic review and meta-analysis. *J Clin Endocrinol Metab* 99(4):1253–1263. <https://doi.org/10.1210/jc.2013-2928>
76. Wienke JR, Chong WK, Fielding JR, Zou KH, Mittelstaedt CA (2003) Sonographic features of benign thyroid nodules: interobserver reliability and overlap with malignancy. *J Ultrasound Med* 22(10):1027–1031
77. Moon WJ, Jung SL, Lee JH, Na DG, Baek JH, Lee YH et al (2008) Benign and malignant thyroid nodules: US differentiation—multicenter retrospective study. *Radiology* 247(3):762–770. <https://doi.org/10.1148/radiol.2473070944>
78. Grani G, Lamartina L, Cantisani V, Maranghi M, Lucia P, Durante C (2018) Interobserver agreement of various thyroid imaging reporting and data systems. *Endocr Connect* 7(1):1–7. <https://doi.org/10.1530/EC-17-0336>
79. Friedrich-Rust M, Meyer G, Dauth N, Berner C, Bogdanou D, Herrmann E et al (2013) Interobserver agreement of thyroid imaging reporting and data system (TIRADS) and strain elastography for the assessment of thyroid nodules. *PLoS ONE* 8(10):e77927. <https://doi.org/10.1371/journal.pone.0077927>
80. Cheng SP, Lee JJ, Lin JL, Chuang SM, Chien MN, Liu CL (2013) Characterization of thyroid nodules using the proposed thyroid imaging reporting and data system (TI-RADS). *Head Neck* 35(4):541–547. <https://doi.org/10.1002/hed.22985>
81. Russ G, Royer B, Bigorgne C, Rouxel A, Bienvenu-Perrard M, Leenhardt L (2013) Prospective evaluation of thyroid imaging reporting and data system on 4550 nodules with and without elastography. *Eur J Endocrinol* 168(5):649–655
82. Park SH, Kim SJ, Kim EK, Kim MJ, Son EJ, Kwak JY (2009) Interobserver agreement in assessing the sonographic and elastographic features of malignant thyroid nodules. *AJR Am J Roentgenol* 193(5):W416–423. <https://doi.org/10.2214/AJR.09.2541>
83. Ragazzoni F, Deandrea M, Mormile A, Ramunni MJ, Garino F, Magliona G et al (2012) High diagnostic accuracy and interobserver reliability of real-time elastography in the evaluation of thyroid nodules. *Ultrasound Med Biol* 38(7):1154–1162. <https://doi.org/10.1016/j.ultrasmedbio.2012.02.025>
84. Friedrich-Rust M, Romenski O, Meyer G, Dauth N, Holzer K, Grunwald F et al (2012) Acoustic radiation force impulse-imaging for the evaluation of the thyroid gland: a limited patient feasibility study. *Ultrasonics* 52(1):69–74. <https://doi.org/10.1016/j.ultras.2011.06.012>
85. Grazhdani H, Cantisani V, Lodise P, Di Rocco G, Proietto MC, Fioravanti E et al (2014) Prospective evaluation of acoustic radiation force impulse technology in the differentiation of thyroid nodules: accuracy and interobserver variability assessment. *J Ultrasound* 17(1):13–20. <https://doi.org/10.1007/s40477-013-0062-5>
86. Zhang YF, Xu HX, He Y, Liu C, Guo LH, Liu LN et al (2012) Virtual touch tissue quantification of acoustic radiation force impulse: a new ultrasound elastic imaging in the diagnosis of thyroid nodules. *PLoS ONE* 7(11):e49094. <https://doi.org/10.1371/journal.pone.0049094>
87. Lam AC, Pang SW, Ahuja AT, Bhatia KS (2016) The influence of precompression on elasticity of thyroid nodules estimated by ultrasound shear wave elastography. *Eur Radiol* 26(8):2845–2852. <https://doi.org/10.1007/s00330-015-4108-2>
88. Vachutka J, Sedlackova Z, Furst T, Herman M, Herman J, Salzman R et al (2018) Evaluation of the effect of tissue compression on the results of shear wave elastography measurements. *Ultrasound Imaging* 40(6):380–393. <https://doi.org/10.1177/0161734618793837>
89. Szczepanek-Parulska E, Wolinski K, Stangierski A, Gurgul E, Ruchala M (2014) Biochemical and ultrasonographic parameters

- influencing thyroid nodules elasticity. *Endocrine* 47(2):519–527. <https://doi.org/10.1007/s12020-014-0197-y>
90. Lyshchik A, Higashi T, Asato R, Tanaka S, Ito J, Hiraoka M et al (2005) Elastic moduli of thyroid tissues under compression. *Ultrasound Imaging* 27(2):101–110
91. Xue Y, Yao S, Li X, Zhang H (2017) Benign and malignant breast lesions identification through the values derived from shear wave elastography: evidence for the meta-analysis. *Oncotarget* 8(51):89173–89181. <https://doi.org/10.18632/oncotarget.21124>
92. Woo S, Suh CH, Kim SY, Cho JY, Kim SH (2017) Shear-Wave Elastography for detection of prostate cancer: a systematic review and diagnostic meta-analysis. *AJR Am J Roentgenol* 209(4):806–814. <https://doi.org/10.2214/AJR.17.18056>
93. Dhyani M, Grajo JR, Bhan AK, Corey K, Chung R, Samir AE (2017) Validation of shear wave elastography cutoff values on the supersonic Aixplorer for practical clinical use in liver fibrosis staging. *Ultrasound Med Biol* 43(6):1125–1133. <https://doi.org/10.1016/j.ultrasmedbio.2017.01.022>

Publisher's Note Springer Nature remains neutral with regard to jurisdictional claims in published maps and institutional affiliations.